NUMERICAL AND EXPERIMENTAL STUDY OF A FLOW OVER STRAIGHT AND SWEPT HIGH-LIFT WINGS

Rumyantsev Andrey, Silantyev Vladimir FSUE "SibNIA named after S.A. Chaplygin", Russian Federation Andrew_CFD@mail.ru, NIO1@sibnia.ru

1 Introduction

High-lift device analysis can be based only on the most comprehensive aerodynamics equations — the Navier-Stokes equations with some models of turbulence. This is explained by complex nature of flow over high-lift wing, in which different kinds of flow separation are observed in the whole range of attack angles.

Previous studies [1] (in the low-speed open-jet wind tunnel T-203 SibNIA on straight (unswept) high-lift wing sections) showed that only some turbulence models (in particular Spalart-Allmaras models and k- ω SST) [1] are the most suitable for these complex problems solving. For all that, the Spalart-Allmaras model provides better matching with

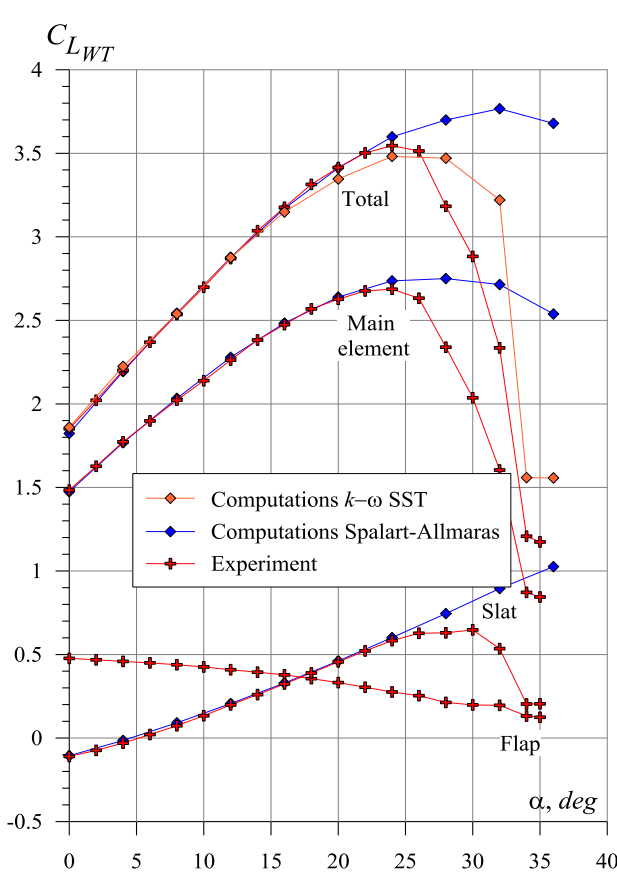


Fig.1. Comparison of computation and experiment (in a coordinate system of a wind tunnel); M=0.12, $R=1.1\cdot10^6$, $\delta_{slat}=30^\circ$, $\delta_{flap}=35^\circ$

experiment to near-critical angles of attack (Fig. 1).

However, it should be noted that at nearand supercritical angles of attack there is a noticeable difference computational and experimental results. Using of empirical criteria (experimental value maximum suction on the slat — $C_{p \, min}$) allows to reduce significantly this angle of attack and value of $C_{L \, max}$ difference.

It should be noted that stall nonuniformity spanwise the wing section at the near- and supercritical angles of attack has noticeable influence on aerodynamics characteristics. This is due to instability of two-dimensional separations in a range of supercritical angles of attack and the formation of three-dimensional periodic separation structure [2].

We should pay attention to one more three-dimensional effect — sweep effect (slipping). The theory of oblique wing is developed for ideal (non-viscous) liquid. However, experiments show that it works also well for viscous flows when there are no large-scale separations. However, for high-lift wings this area of all others is of the greatest interest.

As the analysis shows, experimental studies of swept wing sections at high angles of attack prove to be incorrect. It is caused by strong influence of the so-called middle effect.

Some studies investigate the sweep effect on finite span swept wings or rectangular yawed wings of finite span. However, in the first case the slip effect is difficult to identify because of the strong median and end effects, and in the second case — because of even stronger influence of the end effect of the advancing part of wing located upstream. In this case, the vortex system from the side and front edges completely converts the flow pattern over a wing.

In computational studies, the problem of middle effect to some extent can be eliminated by setting up special boundary conditions in the end sections of the wing box. It allows checking of the swept wing theory on the basis of the numerical experiment. Nevertheless, at nearand supercritical angles of attack, as we know, the accuracy of calculations decreases. Therefore, the experimental check of the computational method is necessary.

The results are presented and the analysis of comparison of numerical and experimental data obtained for a straight and swept finitespan high-lift wing in the conditions of a flow in the wind tunnel T-203 SIBNIA is given in the work.

These results can be useful both in the flow analysis, and in the optimization of high-lift wings.

2 Validation of Turbulence Model for High-Lift Airfoils

The comparison of computation data with the Spalart-Allmaras turbulence model and experimental data for the airfoil on test by the method described in [1] has been carried out. This step is necessary for correct analysis of the slip effect on aerodynamic characteristics of the swept wing section, presented in the following paragraph, and for confirmation of earlier results for high-lift airfoils.

The tests were carried out in the wind tunnel T-203 SIBNIA with an open test section on the straight high-lift wing.

The test wing section was located between two big vertical plates (screens) which vertically exceeded the bounds of the wind tunnel jet.

Flap and slat angles for this wing configuration and the following ones made — $\delta_{slat} = 30^{\circ}$ и $\delta_{flap} = 35^{\circ}$.

The operating conditions is: $V_{\infty} = 40$ m/s ($M_{\infty} = 0.12$), Re = 0.83×10⁶. Angle of attack α varied from 0 to 34° in increments of 2°.

The experiment measured the pressure distribution along the chord in the central section of the wing section.

Comparison of calculated and experimental results are usually presented for unbounded flow conditions. For this, special corrections to the data obtained in the wind tunnel are used, and integral forces are calculated taking into account these corrections. In the case of an open-jet wind

tunnel, the nature of corrections is mainly related to the finiteness of a flow and, as a consequence, its turn. Another factor is a significant jet curvature in the area of the test object. Change in the true angle of attack is connected with the first effect, and pressure redistribution along the chord is connected with the second one.

As stated in [1], it is practically impossible to introduce corrections for the boundary effect in the wind tunnel T-203 SibNIA without involving computational methods (besides pressure distribution varies for the same lift coefficient in the unbounded flow over a highlift airfoil and in the open-jet wind tunnel).

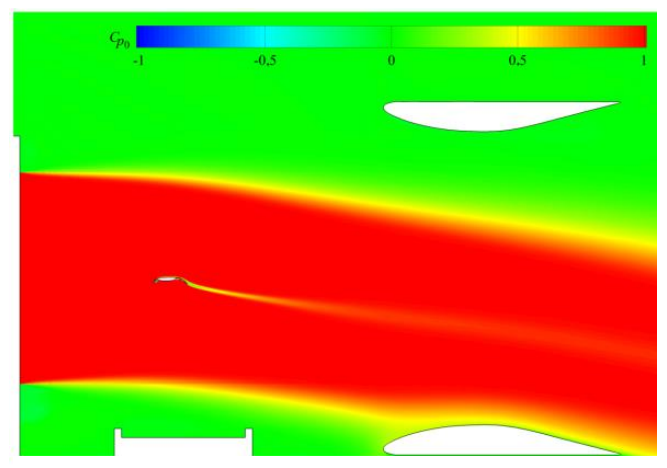


Fig. 2. Simulation of a flow over the airfoil in the open-jet wind tunnel

Therefore, based on this work [1], corrections were not used. All features of the flow over the swept high-lift wing in the test section of the wind tunnel T-203 SibNIA were taken into account in the computation model of two-dimensional "electronic" wind tunnel T-203 SibNIA (Fig. 2).

2.1 Results of Comparison

At $\alpha=0$ (Fig. 3) we can see a divergence of pressure coefficient on the main airfoil nose. This is connected with the flow separation on the lower surface of the slat, which escapes the calculation, namely Spalart-Allmaras turbulence model. While on the other parts of the high-lift airfoil, the pressure is in good agreement with the experiment.

As the angle of attack increases, calculations mostly correctly describe the physical flow pattern as well. In particular, at

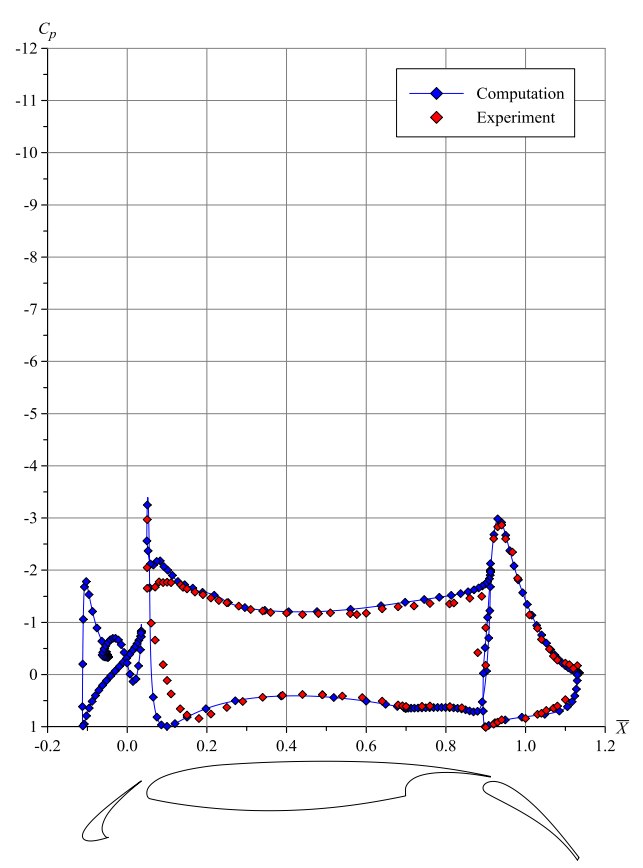


Fig. 3. Comparison of numerical and experimental data; M=0.12, $Re=0.83\cdot 10^6$, $\alpha=0$

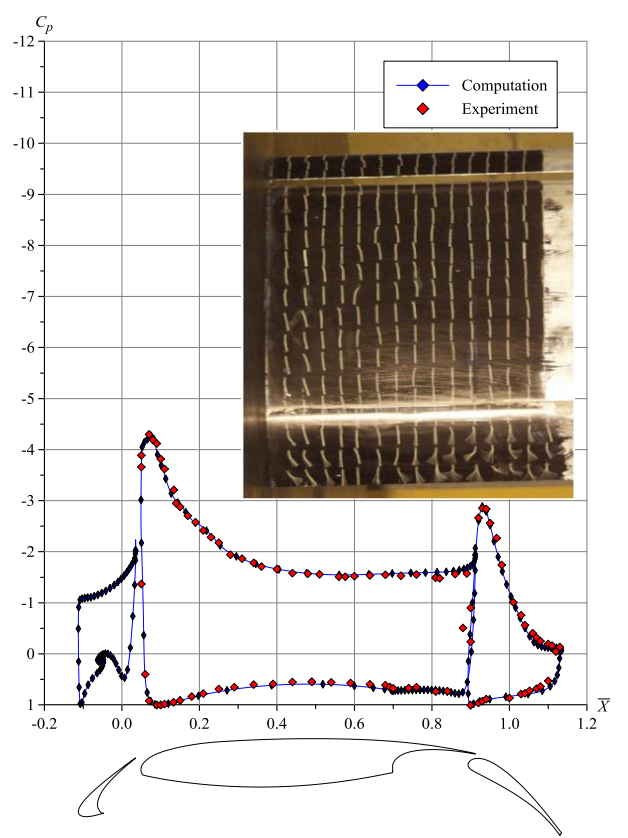


Fig. 4. Comparison of numerical and experimental data; M=0.12, Re=0.83 \cdot 10⁶, α = 10°

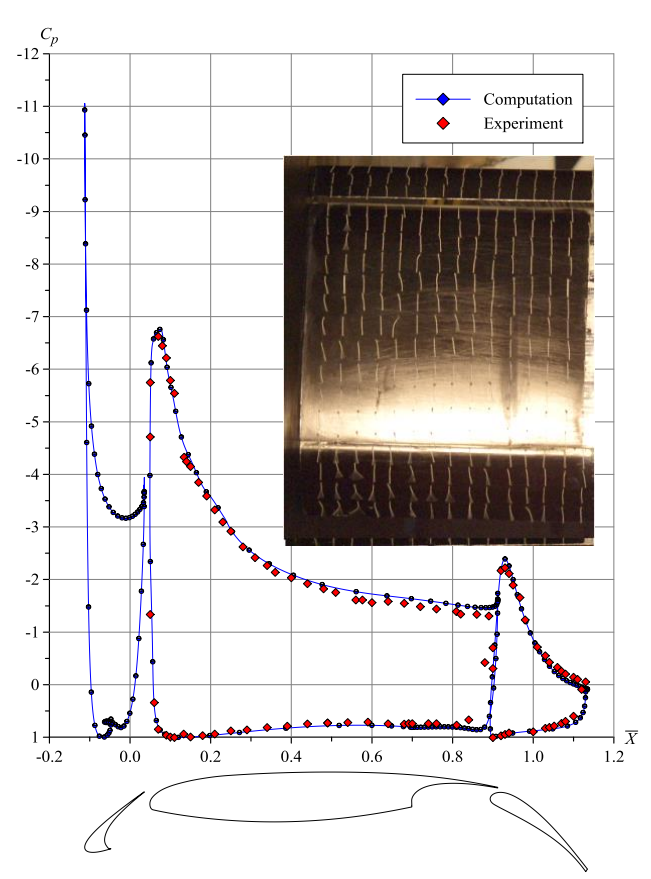


Fig. 5. Comparison of numerical and experimental data; M=0.12, $Re=0.83\cdot10^6$, $\alpha=22^\circ$

moderate angles of attack $\alpha=10^\circ$ in the calculations and spectra of tufts (Fig. 4) a flow separation on the flap is observed. But at the high near-critical angle of attack $\alpha=22^\circ$ (Fig. 5) both in calculations and in spectra of tufts the flow over the flaps becomes the attached one.

At high angles of attack, the results become unreliable, since calculations predict a much later stall. In the experiment, a local flow separation (laminar bubble) occurs on the slat. At angles of attack over 22° it is destroyed, causing global stalling. This factor is not also taken into account by the turbulence model used.

3 Comparison of Two-Dimensional and Three-Dimensional Calculations on Straight and Oblique (Swept) Wings

3.1 The Flow Over the Straight and Oblique Wing Section with High-Lift Devices

Calculations for the straight wing section revealed no special features. Integral forces for this configuration completely coincide with two-dimensional calculation over a whole range of angles of attack (Fig. 6) up to small supercritical α . Even in the presence of separation on the flap at angles of attack 6–8°, there is good agreement.

Let's analyze the slip effect on the aerodynamic characteristics of a multi-element airfoil (normal cross-section of the wing). For this purpose the flow over the section of high-lift wing with the airfoil of modern passenger aircraft in the presence of slip $(\chi=26.6^{\circ})$ was computed.

The results of comparison show that the theory of oblique wing is also valid in general for the high-lift wing streamlined with a slip angle (Fig. 6). Nevertheless, at the same time there are some differences.

Therefore, the influence of large separation zones and flow stagnation zones on the lifting characteristics reduces.

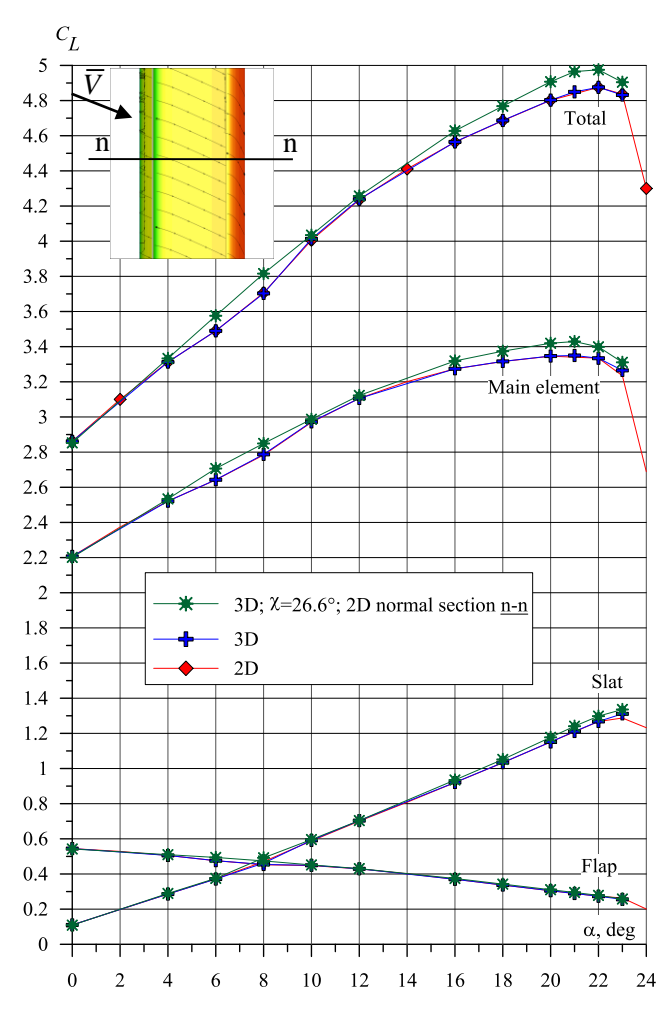


Fig. 6. Comparison of two- and three-dimensional calculation; M=0.18, Re=11.5·10⁶

For example, at the angle of attack $\alpha=8^{\circ}$ (Fig. 7) a reduction of the separation zone sizes on the flap occurs. Apparently this happens due to changing of the flow structure in separation zones (and thus delaying of the flow separation)

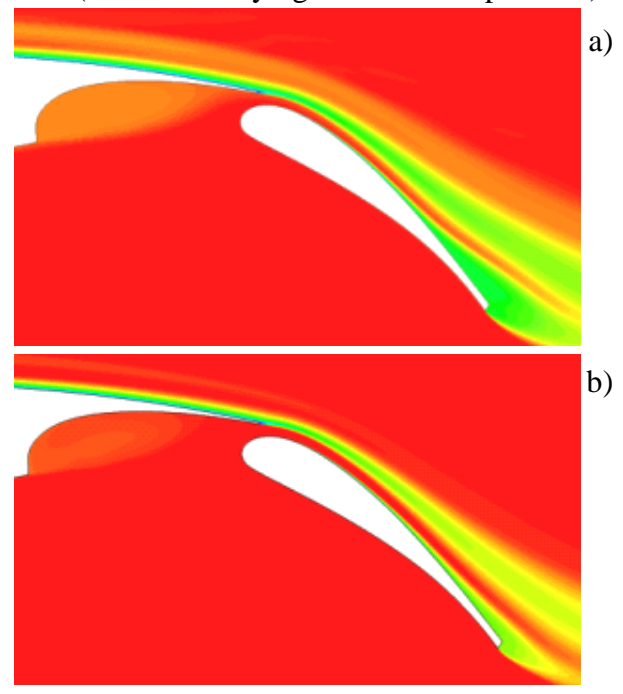


Fig. 7. Field of total pressure coefficient for the case of a flow over a straight (a) and swept (b) wing; M = 0.18, $Re = 11.5 \cdot 10^6$, $\alpha = 8^\circ$

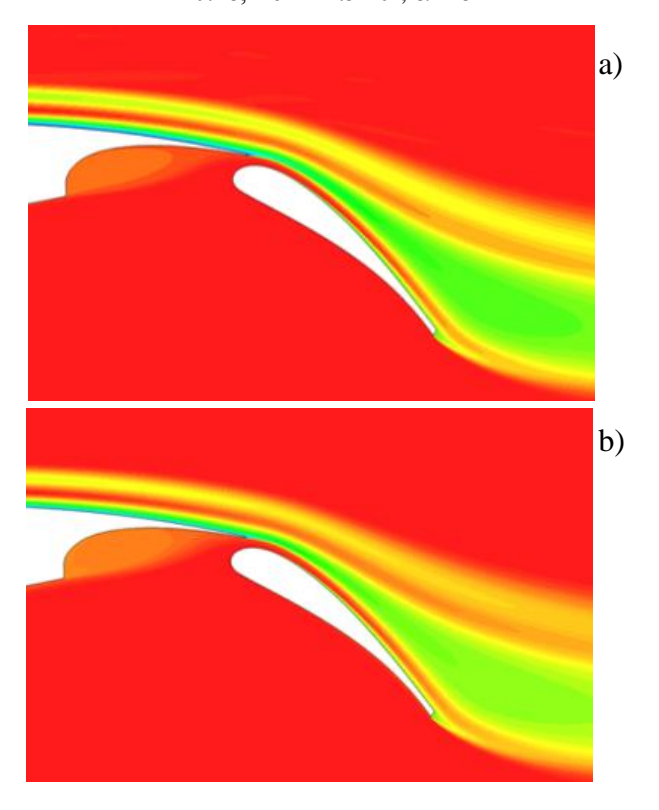


Fig. 8. Field of total pressure coefficient for the case of a flow over a straight (a) and swept (b) wing; M = 0.18, $Re = 11.5 \cdot 10^6$, $\alpha = 17^\circ$

and influence of the cross flow in the stagnation zone.

At high angles of attack $\alpha = 17^{\circ}$ (Fig. 8) in detailed considering, it is possible to notice a slight decrease of the total pressure loss in the flow stagnation zone over the flap, as well as reduction of this zone sizes.

Therefore, the presence of a slip has a positive effect on the flow over the high-lift wing.

4 Comparison of calculation and experiment of the flow over the swept high-lift wing

As indicated above and in the work [1], it is almost impossible to use (boundary corrections in the wind tunnel T-203 SibNIA with an open test section without computation

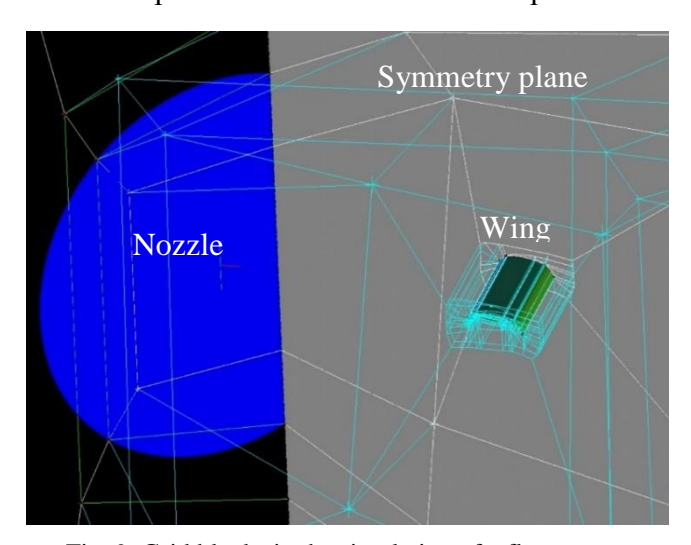


Fig. 9. Grid blocks in the simulation of a flow over a high-lift wing in the conditions of the test section of the wind tunnel T-203 SibNIA

methods.

Therefore, they were not used, and all the features of the flow over the swept high-lift wing in the test section of the wind tunnel T-203 were taken into account in the calculation scheme of the "electronic" wind tunnel T-203 (Fig. 9). The main parameters influencing the distributed and integrated loads are the jet vertical limitation and geometry of the nozzle, whereas supporting devices, the platform, the diffuser etc. have a much smaller impact [1].

In the calculations, given the impact of all parameters, the dimension of the grid will be very large and a number of computer resources required will be far beyond the available. Therefore, in order to simplify the calculation without loss of quality it was proposed to consider the influence of main parameters only.

A slip effect on aerodynamic characteristics of the wing was studied. Calculating possibility when the separation phenomena on the flap were not large was identifying. The experiment was measuring the pressure distribution in the cross-section $\bar{z} = 0.6$, and visualization of a flow over a wing using tufts and oil spectra was carrying out.

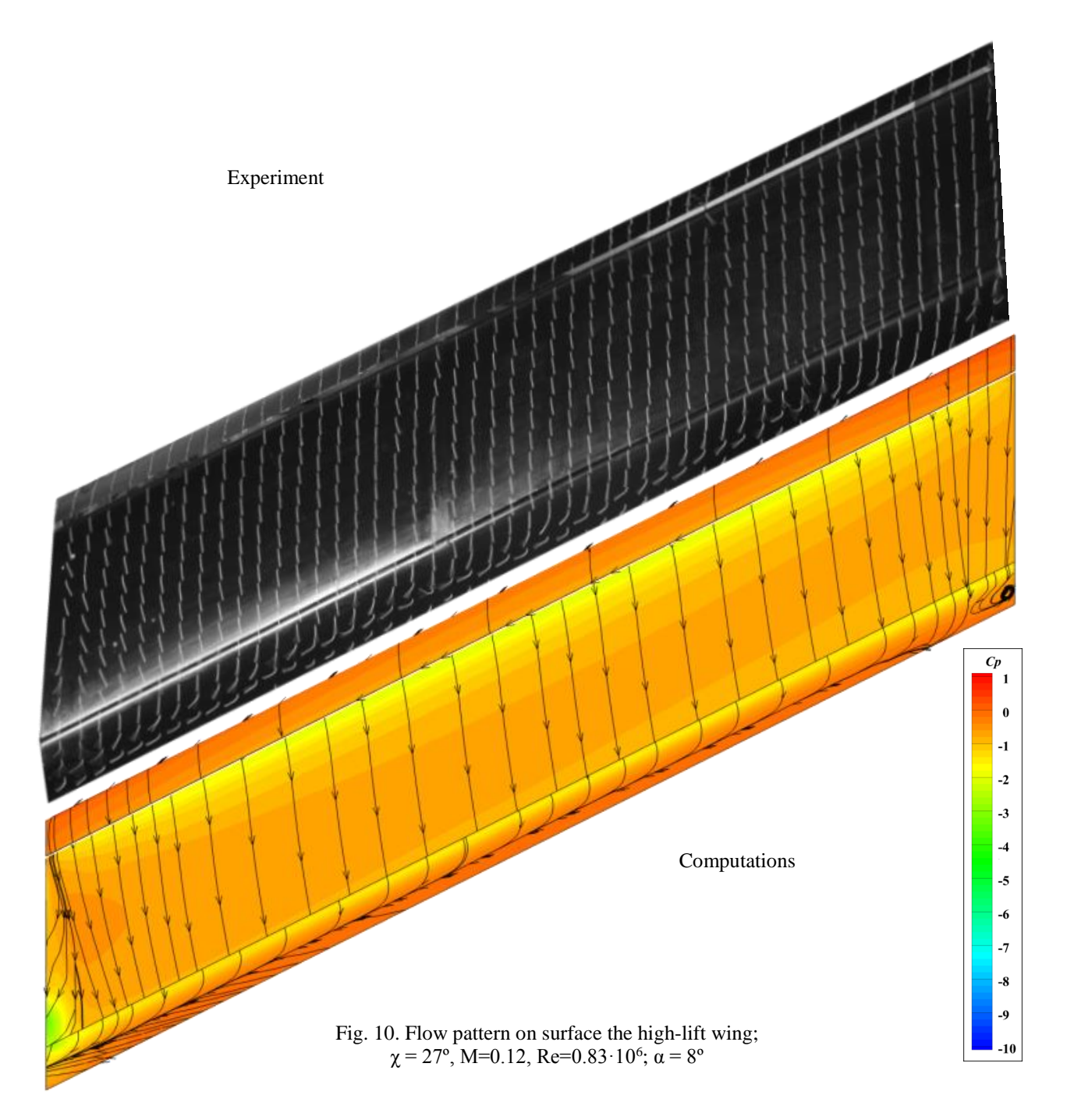
The position of the cross-section was chosen based on specially performed calculations. Computations showed that this wing has a slightly varying distributed load along the span of the wing in the area of a selected cross-section. In addition, a pressure distribution is close in nature to the pressure distribution on the infinite oblique wing. All this allows investigating a slip effect on the characteristics of the wing cross-section both in the calculation and in experiment.

4.1 Results of comparison

Calculations correctly describe the physical flow pattern. In particular, at low angles of attack $\alpha=8^{\circ}$ in the calculations, spectra of tufts and oil spectra (Fig. 10) a weak flow separation on the flap is observed. It can be seen from the photos (Fig. 10) that the periodical structure of the separation on the flap at low angles of attack (characteristic for the straight wing) is practically absent on the swept wing. This demonstrates a slip effect on the separation zones and certain stabilization of the flow.

At the high angle (for example, for the near-critical angle of attack — α = 22°) both in calculations and spectra of tufts (Fig. 11) the flow over the flap becomes the flow without separation.

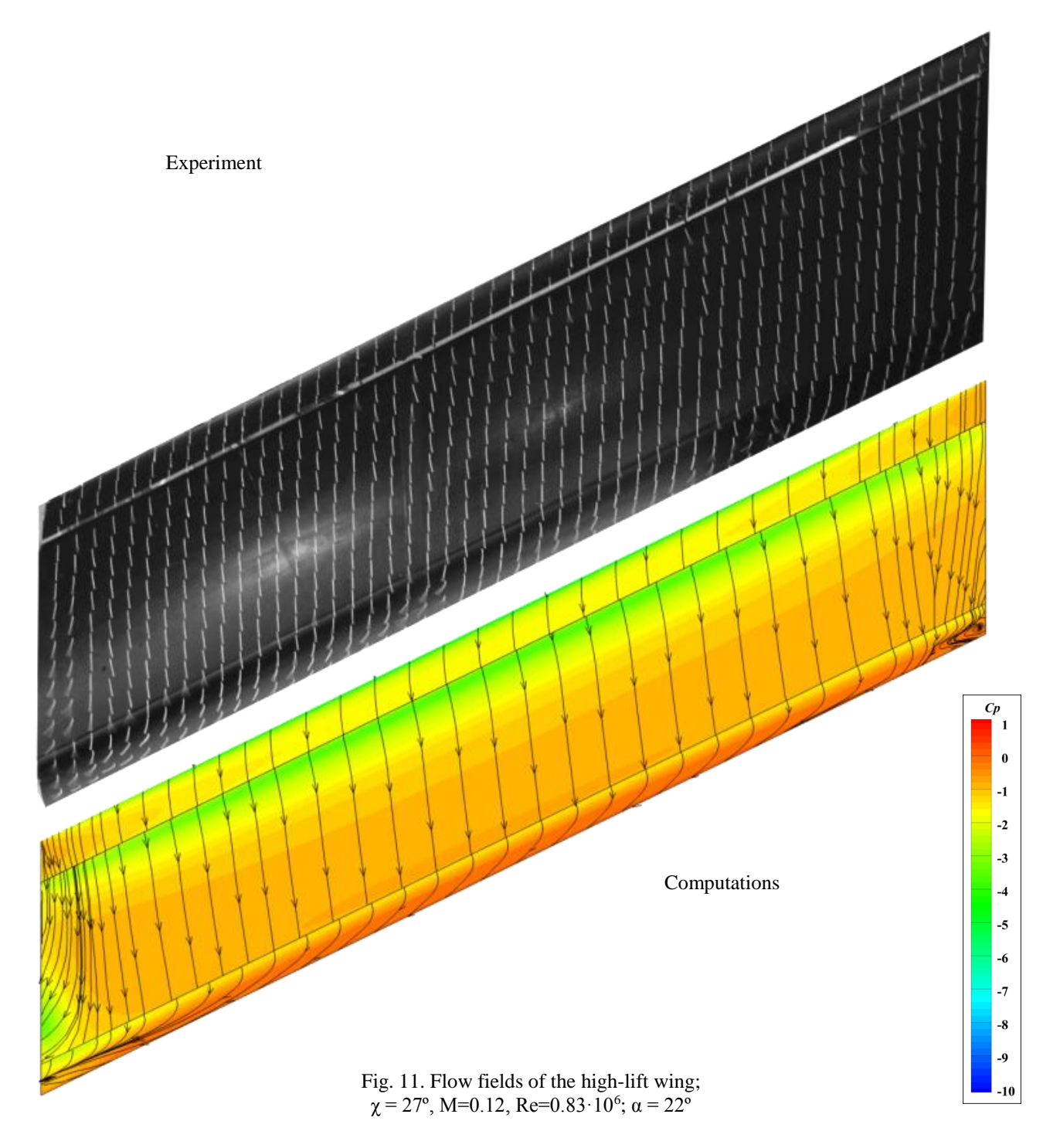
The structure of the flow over the swept wing in calculation is in good qualitative agreement with the experiment (with oil spectra). A good agreement of the pressure coefficient C_p may be noted in a wide range of the attack angle α from 0 up to the critical angle of attack $\alpha = 22^{\circ}$ (Fig. 12,13).



At $\alpha = 22^{\circ}$ (Fig. 13) we have the minimum value of the pressure coefficient $C_p \sim -8.8$. If we calculate it by the value of the normal component of the velocity, then it will become $C_p \sim -11$, which is close to the limit value $C_p = -12$ previously obtained in experiments [1].

At higher angles of attack, the computation results become unreliable — since the calculations predict a much later stall. In the experiment, the laminar bubble on the slat fails and the lift force decreases.

Taking into account the computations of the oblique wing as well as a good agreement of the computation and experiment for the wing section and the swept wing, we can say that the slip positively affects the flow over the swept (oblique) wing.



5 Conclusions

- 1. Computational study based on Navier-Stokes equations with the Spalart-Allmaras turbulence model has been carried out. There is a good agreement of computations on two and three-dimensional schemes on sub- and near-critical angles of attack.
- 2. Study of a flow over a multi-element oblique wing section generally validated the
- correctness of the oblique wing theory for the high-lift wings. Though in this case there is some overestimation of the lift coefficient in the normal section in comparison with the one predicted by the theory and a positive influence of a sliding effect for multi-element wings is shown.
- 3. Computations of a swept finite-span wing showed a good matching with the experiment. The Spalart-Allmaras model describes in a qualitative manner a flow pattern

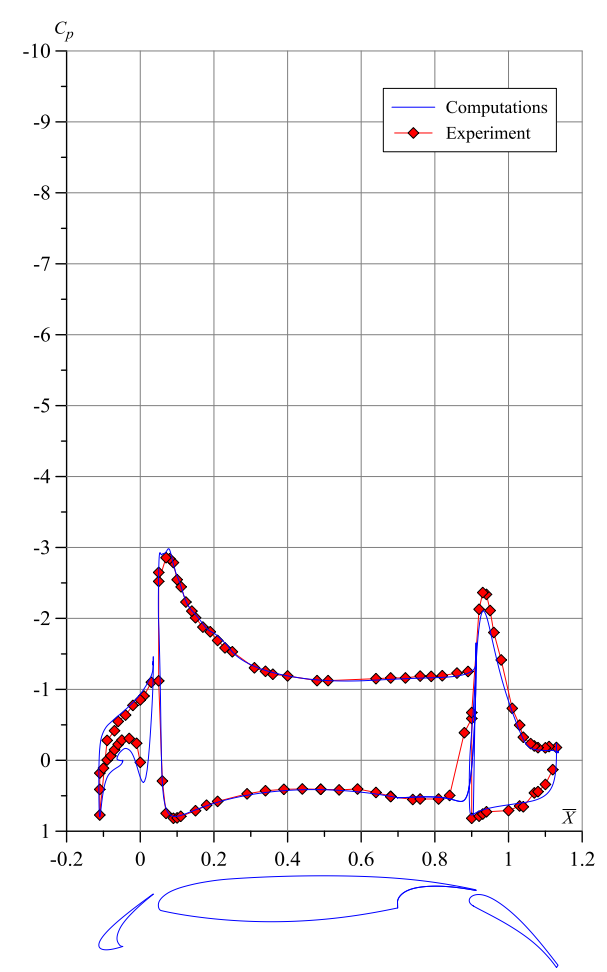


Fig. 12. Comparison of computational and experimental data of a flow over a swept high-lift wing; $\chi = 27^{\circ}$, $\bar{z} = 0.6$, M = 0.12, $Re = 0.83 \cdot 10^{6}$; $\alpha = 8^{\circ}$

over a wing, which is shown by the flow fields. The quantitative matching of the distributed loadings is also presented.

References

- [1] Rumyantsev A.G., Silantyev V.A. *Numerical and Experimental Study of High-Lift Configurations* // Thermophysics and Aeromechanics. 2010. Vol. 17, No. 2. Pp. 91–104.
- [2] Winkelmann A.E., Barlow J.B. Flowfield Model for a Rectangular Planform Wing beyond Stall // AIAA Journal. V. 18. P. 1006–1007.
- [3] Abbot I. H., Doenhoff A. E. *Theory of Wing Sections*. New York: Dover Publications, 1959. 462 p.

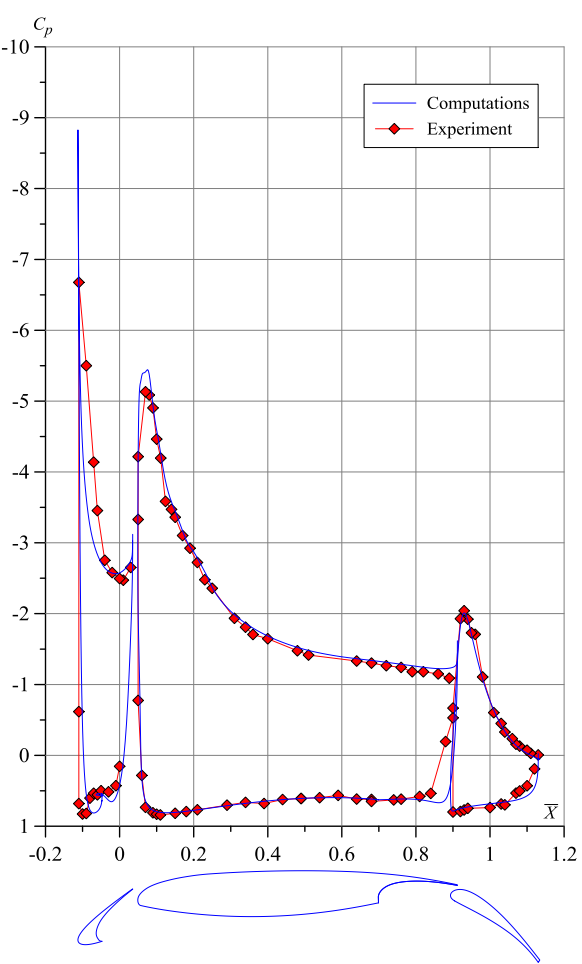


Fig. 13. Comparison of computational and experimental data of a flow over a swept high-lift wing; $\chi = 27^{\circ}$, $\bar{z} = 0.6$, M = 0.12, $Re = 0.83 \cdot 10^{6}$; $\alpha = 22^{\circ}$

Copyright Statement

The authors confirm that they, and/or their company or organization, hold copyright on all of the original material included in this paper. The authors also confirm that they have obtained permission, from the copyright holder of any third party material included in this paper, to publish it as part of their paper. The authors confirm that they give permission, or have obtained permission from the copyright holder of this paper, for the publication and distribution of this paper as part of the ICAS 2014 proceedings or as individual off-prints from the proceedings.